

## Josephson flux-flow resonances in overdamped long $\text{YBa}_2\text{Cu}_3\text{O}_7$ grain-boundary junctions

Y. M. Zhang, D. Winkler, P.-Å. Nilsson, and T. Claeson

Department of Physics, Chalmers University of Technology, S-412 96 Göteborg, Sweden

(Received 21 November 1994)

A resonance structure was observed in the current-voltage curves of overdamped long  $0\text{--}32^\circ$ [001]-tilt  $\text{YBa}_2\text{Cu}_3\text{O}_7$  bicrystal grain-boundary junctions (GBJ's), and is attributed to a Josephson flux-flow resonance. The voltage position of the resonance moves almost linearly from 0.5 to 2 mV with an applied magnetic field. From this linear dependence and using the London penetration depth  $\lambda_L = 140$  nm, we determined the ratio between the effective dielectric thickness and the relative dielectric constant  $t/\epsilon_r \approx 0.3$  nm, and the quasiparticle loss coefficient  $\alpha = 1.3$  at 16 K for a  $30\text{-}\mu\text{m}$  long junction. The loss increases with temperature and no resonance was seen at 77 K. The perturbed sine-Gordon equation was used for modeling long GBJ's. Simulations support the experimental observation that Josephson vortices can propagate unidirectionally in an overdamped, homogeneous junction up to  $\alpha \approx 2$ .

A long Josephson junction (LJJ) has one dimension considerably larger than the size of a Josephson vortex (fluxon) in the junction. Active three-terminal devices based on fluxon motion in LJJ's have been investigated both in low- $T_c$  (Refs. 1–3) and high- $T_c$  (Refs. 4 and 5) superconducting systems. One device that may be useful in space communication, e.g., as the local oscillator in a mixer/receiver, is the Josephson flux-flow oscillator.<sup>2,3</sup> It is based on an *underdamped* LJJ operated in the viscous flux-flow state. In this state, an array of Josephson vortices that is produced by a magnetic field applied in the plane of the junction is driven unidirectionally by a Lorentz force caused by bias current flowing across the junction. Also, an electromagnetic (EM) wave can propagate along the junction and its phase velocity was derived by Swihart.<sup>6</sup> When the fluxon velocity  $u$  approaches the Swihart velocity  $\tilde{c}$ , a current step due to the nonlinear interaction of the fluxon motion with the traveling EM wave appears in the current-voltage ( $I$ - $V$ ) characteristic. This step is often referred to as the Eck peak<sup>7</sup> or the “velocity-matching” (VM) step. The step voltage,  $V_m$ , can be tuned over a wide range by changing the magnetic field. The power of the EM radiation is maximum at  $V_m$ , giving a Josephson frequency,  $f = 2 eV_m/h$ .

A considerable amount of experimental and theoretical work<sup>2,3,8,9</sup> has been devoted to study the flux-flow in LJJ's. However, they are limited to low- $T_c$  junctions, either in *underdamped* superconductor-insulator-superconductor (SIS) tunnel junctions (the quasiparticle loss coefficient  $\alpha$  is within the range of 0.1 to 0.5), or in *overdamped* superconductor-normal-metal-superconductor (SNS) bridge junctions.<sup>10</sup> To our knowledge, no experimental results have been reported on VM steps in high- $T_c$  junctions which are usually overdamped. We report in this paper on the observation of resonance structures in the current-voltage ( $I$ - $V$ ) characteristics of *overdamped* high- $T_c$  grain boundary junctions (GBJ's), which we believe are the VM steps due to Josephson flux flow. This observation may aid in the understanding of the nature of high- $T_c$  grain-boundary interfaces. The finding was supported by numerical simulations that show that Josephson vortices may propagate unidirectionally in an LJJ which is overdamped (i.e.,  $\alpha > 1$ ). We will demonstrate that properties

of a GBJ, such as the intrinsic capacitance  $C$  and the quasiparticle loss  $\alpha$ , can be determined from the magnetic field dependence of the VM step. These parameters are important in the design of three-terminal devices based on fluxon motion in high- $T_c$  junctions.

The junctions were formed by growing 200 nm thick  $\text{YBa}_2\text{Cu}_3\text{O}_{7-\delta}$  (YBCO) thin films on yttria stabilized zirconia (YSZ)  $0\text{--}32^\circ$ , [001]-tilt bicrystals. The GBJ's had resistively shunted-junction (RSJ) like  $I$ - $V$  curves at temperatures up to  $\sim 80$  K. Near the transition temperature, thermally activated phase slippage in the junction gives a noise rounded dc Josephson current.<sup>11</sup> A schematic drawing of a long YBCO bicrystal GBJ is shown in the inset of Fig. 1. The lengths,  $L$ , of the junctions along the grain boundary were 10, 20, 30, and  $40\ \mu\text{m}$ . The junctions are long Josephson junctions because their lengths are much larger than the Jo-

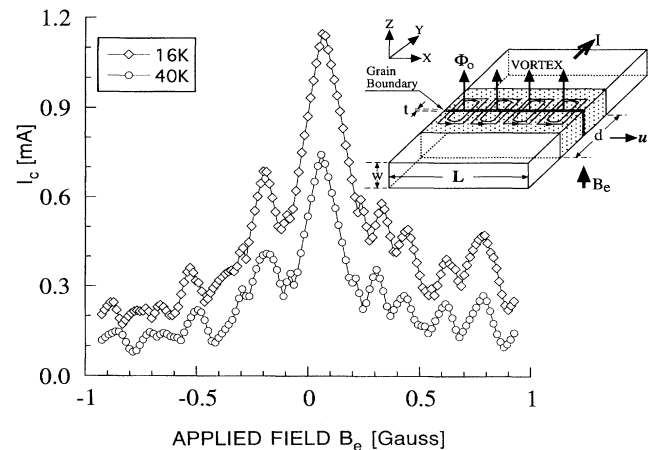


FIG. 1. Critical current  $I_c$  versus applied magnetic field  $B_e$  of a  $30\ \mu\text{m}$  long  $0\text{--}32^\circ$  [001]-tilt GBJ on YSZ at  $T = 16$  and  $40$  K. The inset gives a schematic drawing of a long bicrystal GBJ in YBCO. Josephson vortices penetrate the grain boundary when a field is applied in the plane of the junction ( $+z$  direction). Driven by the Lorentz force caused by the bias current  $I$ , all the vortices move as a vortex array with a speed of  $u$  in the  $+x$  direction.

sephson penetration depth  $\lambda_J = \sqrt{\Phi_0/2\pi\mu_0 j_c d}$ .  $\lambda_J$  determines the extent of a fluxon in the junction. ( $\Phi_0 = h/2e$  is the magnetic flux quantum,  $\mu_0$  the vacuum permeability, and  $j_c$  the critical current density.) It is about  $2 \mu\text{m}$  for a typical  $j_c$  of  $20 \text{ kA/cm}^2$  at around  $16 \text{ K}$  (assuming a uniform current distribution in the junction).

The effective magnetic thickness  $d$  of the junction is equal to  $d = t + 2\lambda_L \approx 2\lambda_L$ , where  $t$  is the junction ‘‘barrier’’ thickness and  $\lambda_L$  is the London penetration depth. We use a value of  $\lambda_L = 140 \text{ nm}$  (for  $T \ll T_c$ ), from the literature<sup>12</sup> (for the YBCO film) and from independent measurements at the grain-boundary interfaces.<sup>13</sup> A magnetic field applied perpendicular to the YBCO film is focused into the junction area.<sup>14</sup> The flux focusing factor  $F$  can be estimated from  $F = \Phi_0 / L\Delta B_e$ . Here,  $\Delta B_e$  is the change in the flux density corresponding to the penetration of one more flux quantum into the junction. For a long junction,  $\Delta B_e$  can be roughly estimated from two nearby dips (some periods away from the center lobe) in the magnetic field dependence of the critical current  $I_c$  (see Fig. 1 for a  $30 \mu\text{m}$  long junction at  $16$  and  $40 \text{ K}$ ). This leads to a focusing factor of  $F = 15 \pm 1$ . In this respect, a bicrystal junction is quite different from a low- $T_c$  sandwich tunnel junction (which has a focusing factor close to 1). As is expected for a long junction,  $I_c$  does not go down to zero with magnetic field. However, the field dependence is asymmetric and has structures that indicate that the current distribution along the junction is not perfectly uniform. This may be due to defects, like high current paths or voids along the grain boundary.

Figure 2 shows the  $I$ - $V$  curves for a  $30 \mu\text{m}$  long ( $L/\lambda_J = 13.6$ ) GBJ (with  $I_c R_n = 1.15 \text{ mV}$  at  $16 \text{ K}$ , and  $0.1 \text{ mV}$  at  $77 \text{ K}$ ) for different applied magnetic fields.  $I_c$  is the critical current and  $R_n$  is the normal state resistance. We observe a field dependent, resonant like current step in the  $I$ - $V$  traces. Since the voltage position of the step depends linearly on the applied field (see the inset of Fig. 2) and is reproducibly seen for several junctions with proper parameters, we relate these steps to the VM steps (for  $u = \bar{c}$ ) caused by unidirectional Josephson flux flow along the grain boundary.

The linear relation [ $V_m(\text{mV}) \approx -0.30 + 4.2B_e(\text{G})$ ] for this GBJ is due to that  $V_m$  depends on the number of Josephson vortices in the junction. Due to high damping in a GBJ, these steps are much less sharp than those in long Nb//NbO<sub>x</sub>/PbBi junctions, see, e.g., Refs. 2 and 3. In order to determine the step voltage  $V_m$  accurately, we subtract the normal current,  $V/R_n$ , from the bias current  $I$  and determine  $V_m$  from the peak of  $\langle I_s \rangle = I - V/R_n$  versus the dc voltage (see Fig. 2). Here,  $\langle I_s \rangle$  represents the space averaged dc supercurrent across the GBJ.  $R_n$  of this junction was about  $1 \Omega$  and almost constant from  $16$  to  $80 \text{ K}$ .  $I_c$  was  $1.15 \text{ mA}$  at  $16 \text{ K}$  and it decreased almost linearly with increasing temperature ( $110 \mu\text{A}$  at  $77 \text{ K}$ ). The voltage range ( $0.5$  to  $2 \text{ mV}$  for this junction) corresponds to Josephson frequencies ranging from about  $250$  to  $1000 \text{ GHz}$ . The upper voltage limit is approximately equal to  $2I_c R_n$  at  $16 \text{ K}$ . We also observe (Fig. 2) that the VM step becomes smaller and wider at a higher voltage. This is expected from the increasing surface losses inside the GBJ at higher frequency.

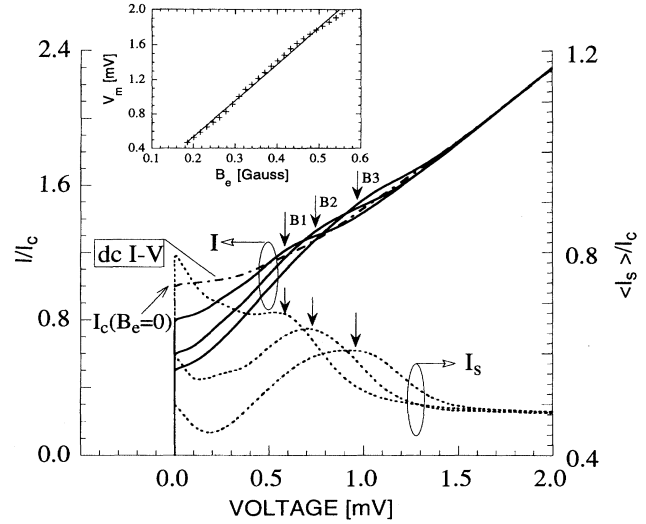


FIG. 2. Magnetic field response of a  $30 \mu\text{m}$  long GBJ at  $T = 16 \text{ K}$ . The dc  $I$ - $V$  curve has the maximum critical current  $I_c = 1.15 \text{ mA}$  at no magnetic field. The  $I/I_c$  vs  $V$  curves as well as  $\langle I_s \rangle/I_c$  vs  $V$  curves correspond to increasing applied fields: B1 ( $=0.20 \text{ G}$ ), B2 ( $=0.25 \text{ G}$ ), and B3 ( $=0.29 \text{ G}$ ). The inset shows the flux-flow step voltage  $V_m$  versus applied magnetic field  $B_e$  of this junction. These data can be linearly fitted by  $V_m(\text{mV}) = -0.30 + 4.2B_e(\text{G})$ . Note that the linear curve yields a negative intercept for zero field. This is caused by the self-field in the experiment and was not taken into account in Eq. (1).

Excess current  $I_{\text{ex}} (= I - V/R_n)$ , i.e., the time-average supercurrent for  $V \gg I_c R_n$ , is sometimes observed in our junctions and can be seen in Fig. 2. Several mechanisms have been suggested to give excess current. The most common explanation has been Andreev reflections at a superconductor and/or normal material interface. However, as reported in Ref. 15, this mechanism can be destroyed with the presence of a dielectric barrier. Our measurements on other high quality bicrystal GBJ's show clear hysteretic  $I$ - $V$  curves (i.e., these junctions are underdamped with  $\alpha < 1$ ) at temperatures below  $14 \text{ K}$ . These junctions have very little excess current ( $I_{\text{ex}}/I_c < 0.1$ ) and display pronounced Josephson flux flow, and Fiske resonances within the same junction.<sup>16</sup>  $I_c$  of these junctions also shows a much better dependence on the applied field. Another possible mechanism for the excess current is a nonsinusoidal or multivalued current-phase relation<sup>17</sup> of a high- $T_c$  junction. However, measurements on oxygen-ion irradiated<sup>18</sup> and step edge<sup>19</sup> junctions show a standard sinusoidal current-phase relation. From our measurements on many GBJ's on different YSZ bicrystals, we conjecture that, depending on the processing procedure in making a bicrystal GBJ, the excess current can be either very small (more SIS-like barrier) or higher. The interface at the bicrystal itself could be very crucial for the junction properties. Since many of our long GBJ's have  $\alpha > 1$  at  $16 \text{ K}$ , we concentrate on flux flow in overdamped junctions in this paper. The detailed nature of the boundary region will not be addressed here. However, we will argue that the barrier (and/or boundary) effectively is dielectric in its nature.

Electromagnetic properties of a long GBJ can be deter-

mined from the dependence of the VM step on the applied magnetic field, if we assume that the model for low- $T_c$  tunnel junctions (with barrier capacitances) can be used for GBJ's. Taking into account the flux focusing effect in the junction area, the VM-step voltage (for  $u=\bar{c}$ ) is related to the applied flux density  $B_e$  as:<sup>9</sup>

$$V_m = d\bar{c}FB_e, \quad (1)$$

where the Swihart velocity of an EM wave propagating along the junction is  $\bar{c} = c_0(t/\epsilon_r d)^{-1/2}$ , and  $c_0$  is the light velocity in vacuum.

Using our previously extracted value of  $F \approx 15$  and  $dV_m/dB_e = 4.2$  mV/G (Fig. 2), we obtain  $\bar{c} \approx 9.7 \times 10^6$  m/s. With  $\lambda_L = 140$  nm (Refs. 12 and 13) the value of  $\bar{c}$  corresponds to  $t/\epsilon_r = 0.29 \pm 0.04$  nm, which represents the *average* ratio of the barrier (and/or boundary) thickness and the relative dielectric constant between the grains of a YBCO GBJ on a 0–32° [001]-tilt YSZ bicrystal. This value is consistent with  $t/\epsilon_r \approx 0.4$  nm, which was determined separately from Fiske modes in a GBJ having an order of magnitude lower  $j_c$ .<sup>13</sup> With  $t/\epsilon_r = 0.29 \pm 0.04$  nm, the intrinsic capacitance per unit area becomes  $C = 30 \pm 4$  fF/ $\mu\text{m}^2$ . The thickness of the YBCO film (200 nm) is much larger than that of the barrier and/or boundary [e.g.,  $t \approx 1.5$  nm, using  $\epsilon_r = 5$  for oxygen deficient YBCO (Ref. 20)], and the stray capacitance  $C_s$  through the YSZ substrate ( $\epsilon_r \approx 25$ ) can be ignored<sup>21</sup> (within the error bar of the estimated  $t/\epsilon_r$ ).

The junction intrinsic capacitance is an important parameter for evaluating the high frequency properties at the grain boundary. For example, the quasiparticle loss  $\alpha$  can be calculated from the expression<sup>9</sup>

$$\alpha = (1/I_c R_n)(j_c \Phi_0 / 2\pi C)^{1/2}. \quad (2)$$

It is clear from Eq. (2) that a very small  $C$  will lead to an infinite quasiparticle loss, no EM wave can propagate in the junction and, hence, no flux-flow can be sustained.<sup>22</sup> For this sample, we get  $\alpha = 1.3$  at 16 K. Similar resonances were observed for 10, 20, and 40  $\mu\text{m}$  long junctions. The  $\alpha$  value of 1.3 value shows that our long GBJ is *overdamped*. It is much higher than the typical values of  $\alpha = 0.1$  to 0.5 in low- $T_c$  Josephson tunnel junctions.<sup>2,3</sup> Hence, our observations of VM steps in these GBJ's show that a Josephson vortex array can propagate also in an *overdamped* junction. For a given junction with  $R_n$  and  $C$  constant, we see from relation (2) that  $\alpha$  is proportional to  $j_c^{-1/2}$ . For our 30  $\mu\text{m}$  long junction,  $j_c(16 \text{ K})/j_c(77 \text{ K}) \approx 10$ . This leads to as high a loss as  $\alpha \approx 4.1$  at 77 K and may explain the absence of VM steps at such a high temperature.

Numerical simulations usually provide more information on the dynamics of a LJJ, especially the time and space distributions of the EM field in the junction. For a high- $T_c$  GBJ, it is an open question whether the model developed for a low- $T_c$  LJJ is applicable. Assuming (a) a homogeneous bias current and critical current density along the junction; (b) a sinusoidal current-phase relation; (c) a nonzero intrinsic junction capacitance  $C$ , we may model the dynamics of Josephson vortices in a long GBJ by the perturbed sine-Gordon equation (see, e.g., Ref. 23)

$$\phi_{xx} - \phi_{tt} - \sin\phi = \alpha\phi_t - \beta\phi_{xxt} - \gamma. \quad (3)$$

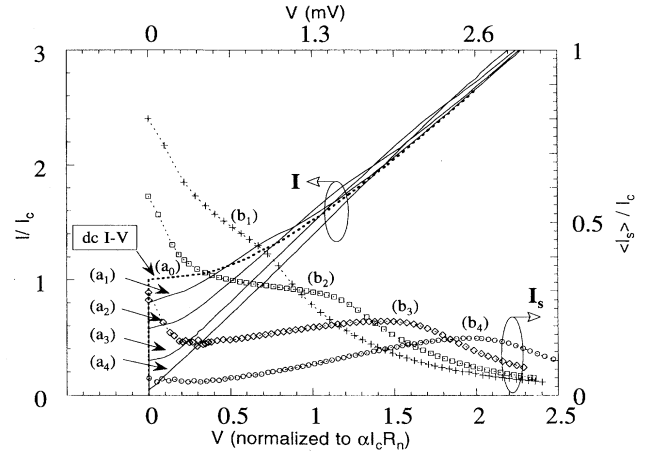


FIG. 3. Simulation of the normalized  $I$ - $V$  curves ( $a_0$ – $a_4$ ), and the normalized  $\langle I_s \rangle$  vs  $V$  curves ( $b_1$ – $b_4$ ) of a LJJ at different applied fields:  $\beta_e = 0$  ( $a_0$ ), 0.5 ( $a_1$  and  $b_1$ ), 1.0 ( $a_2$  and  $b_2$ ), 1.5 ( $a_3$  and  $b_3$ ), and 2 ( $a_4$  and  $b_4$ ). Parameters are  $L/\lambda_J = 14$ ,  $\alpha = 1.3$ , and  $\beta = 0.001$ . Voltages that would correspond to the 30  $\mu\text{m}$  junction are also shown on the top  $x$  axis.

$\phi(x, t)$  is the superconducting phase difference between the electrodes, the spatial coordinate  $x$  is normalized to  $\lambda_J$ , and time  $t$  is normalized to the inverse plasma frequency,  $1/2\pi f_J$ .  $\beta$  represents surface loss in the electrodes, and  $\gamma$  is the normalized bias current ( $I/I_c$ ). For a junction with normalized length  $l = L/\lambda_J$ , the boundary conditions are determined by  $\phi_x(X_L, t) + \beta\phi_{xt}(X_L, t) = -\beta_e$  ( $X_L = 0$  or  $l$ ). The constant  $\beta_e (= B_e/\mu_0\lambda_J j_c)$  is the normalized applied magnetic field. The voltage is normalized to  $V_J (= \Phi_0 f_J \approx \alpha I_c R_n)$ . For simplicity, the flux focusing effect and the self-field are not taken into account in the simulation.

Simulations confirm that the viscous flux-flow mode can be excited in an overdamped long junction. Figure 3 shows the bias current and the space averaged dc supercurrent  $\langle I_s \rangle$  versus the dc voltage, calculated at different magnetic fields. In order to compare with experimental data,  $\alpha = 1.3$  and  $L/\lambda_J = 14$  are used in the calculation. For simplicity, we assume the surface loss  $\beta$  is a constant (0.001). We see that the VM-step voltage increases, and the critical current decreases, with the applied field. The number of vortices in the junction is given by  $\Phi/\Phi_0 = \beta_e l/2\pi$  (assuming the self-field from the bias current can be ignored). When the field  $\beta_e \leq 1$ , only weak traces from the flux flow can be seen in the  $\langle I_s \rangle$  vs  $V$  curve and the supercurrent  $I_c$  is only partially suppressed. This is because the vortices can only occupy part of the junction at such weak fields. A more clear resonant step exists when  $\beta_e = 1.5$ . At a larger field  $\beta_e = 2$ ,  $I_c$  is suppressed to almost zero and vortices completely penetrate the junction barrier. The shapes of the resonant steps are similar in experiment and simulation. Taking into account that the voltages in the simulation are normalized to  $\alpha I_c R_n$  ( $\approx 1.4$  mV for the 30  $\mu\text{m}$  junction at 16 K), normalized resonant voltages of 0.7 (for  $\beta_e = 0.5$ ) to 2 (for  $\beta_e = 2$ ) translate into real voltages of 1 to 2.8 mV. Compared with the experimental data, from 0.5 to 2 mV, the simulation gives a higher voltage range. Recent simulations<sup>16</sup> introducing “a low-current-path” of size  $\lambda_J$  near one end of the junction where the

vortices enter gives a comparable shift downward of the VM-step voltage, i.e., the VM steps start to appear at lower fields ( $\beta_e < 0.5$ ). Also, simulation shows that the existence of a finite surface loss  $\beta$  ( $> 0.01$ ) can also decrease the voltage of a VM step. For example, the normalized voltage for a VM step decreases from 1.93 to 1.74, for  $\beta$  changing from 0.01 to 0.1. There are almost no influences from the  $\beta$  value if it is smaller than 0.01, for the bias region studied here.

We also simulate the dependence of  $\langle I_s \rangle$  with bias voltage for different dampings:  $\alpha = 0.65$  (underdamped), 1.3 (overdamped), and 2 (strongly overdamped). Similar parameters as in Fig. 3 are used for this simulation ( $L/\lambda_J = 14$ ,  $\beta = 0.001$ ), with fields  $\beta_e = 1.5$  and 2. Results show that a smaller  $\alpha$  gives a higher and sharper resonance.  $V_m$  decreases with increasing  $\alpha$ , especially at the low field ( $\beta_e = 1.5$ ). For the underdamped case,  $\alpha = 0.65$ , the VM step shows a clear switch from the flux-flow resonance at  $u = \bar{c}$  to the almost zero-fluxon oscillation<sup>9</sup> at  $u > \bar{c}$ . This latching is lost for the overdamped junction with  $\alpha = 1.3$  (corresponds to the  $\alpha$  value in our experiment). The simulation suggests that for a long junction of  $l = 14$ , the flux flow is difficult to sustain and VM steps are difficult to observe if the damping  $\alpha > 2$ .

In conclusion, we observed magnetic field dependent velocity-matching resonant steps, that are generated by Josephson flux flow in long YBCO grain boundary junctions on YSZ bicrystals. These steps were observed from 0.5 to 2.0

mV in a 30  $\mu\text{m}$  long overdamped junction at 16 K. The upper voltage limit for observing a VM step is approximately equal to  $2I_c R_n$ . The presence of VM steps supports the picture<sup>13</sup> that the GBJ is formed around a dielectriclike barrier and/or boundary between superconducting grains and/or electrodes, possibly nonuniform but constituting a sufficiently high  $Q$  value transmission line to propagate EM waves. The variation of the VM-step voltage with magnetic field can be used to extract parameters of GBJ's over a wide frequency range, using a model developed for low- $T_c$  tunnel junctions. For a typical 30  $\mu\text{m}$  long GBJ at 16 K (which has  $L/\lambda_J = 13.6$ ), we determined  $\bar{c} = 9.7 \times 10^6$  m/s,  $t/\epsilon_r \approx 0.3$  nm,  $C \approx 30$  fF/ $\mu\text{m}^2$ , and  $\alpha = 1.3$ . Simulations confirm that flux flow is possible in an overdamped Josephson junction with parameters corresponding to the experiment ( $\alpha = 1.3$  and  $L/\lambda_J = 14$ ). The simulation also provides reasonable agreement with the experiment on the shape of flux-flow steps. The Josephson flux flow is strongly affected by the  $\alpha$  value. It vanishes for  $\alpha > 2$ .

Stimulating discussions with N. F. Pedersen, E. Wikborg, A. Ustinov, A. Yurgens, G. Wendin, and S. Pagano are acknowledged. E. A. Stepantsov supplied the bicrystal substrate. This work was performed within the ESPRIT basic research project no. 7100 and the NORdic Program for Applied Superconductivity. The Swedish Nanometer Laboratory was utilized.

- 
- <sup>1</sup>T. J. Rajeevakumar, Appl. Phys. Lett. **39**, 439 (1981).  
<sup>2</sup>T. Nagatsuma, K. Enpuku, F. Irie, and K. Yoshida, J. Appl. Phys. **54**, 3302 (1983).  
<sup>3</sup>Y. M. Zhang and D. Winkler, IEEE Trans. Microwave Theory Tech. **42**, 726 (1994).  
<sup>4</sup>L. Alff *et al.*, J. Appl. Phys. **75**, 1843 (1994).  
<sup>5</sup>Y. M. Zhang, D. Winkler, P. Å. Nilsson, and T. Claeson, Appl. Phys. Lett. **64**, 1153 (1994).  
<sup>6</sup>J. C. Swihart, J. Appl. Phys. **32**, 461 (1961).  
<sup>7</sup>R. E. Eck, D. J. Scalapino, and B. N. Taylor, Phys. Rev. Lett. **13**, 15 (1964).  
<sup>8</sup>A. V. Ustinov *et al.*, IEEE Trans. Appl. Supercond. **3**, 2287 (1993).  
<sup>9</sup>Y. M. Zhang, Ph.D. thesis, Chalmers University of Technology, Göteborg, Sweden, 1993.  
<sup>10</sup>J. R. Waldram, A. B. Pippard, and J. Clarke, Philos. Trans. R. Soc. London Ser. A **268**, 265 (1970).  
<sup>11</sup>R. Gross, P. Chaudhari, D. Dimos, A. Gupta, and G. Koren, Phys. Rev. Lett. **64**, 228 (1990).  
<sup>12</sup>M. C. Nuss, K. W. Goossen, P. M. Mankiewich, and M. L. O'Malley, Appl. Phys. Lett. **58**, 2561 (1991).  
<sup>13</sup>D. Winkler, Y. M. Zhang, P. Å. Nilsson, E. A. Stepantsov, and T. Claeson, Phys. Rev. Lett. **72**, 1260 (1994).  
<sup>14</sup>P. A. Rosenthal, M. R. Beasley, K. Char, M. S. Colclough, and G. Zaharchuk, Appl. Phys. Lett. **59**, 3482 (1991).  
<sup>15</sup>G. E. Blonder, M. Tinkham, and T. M. Klapwijk, Phys. Rev. B **25**, 4515 (1982).  
<sup>16</sup>Y. M. Zhang *et al.* (unpublished).  
<sup>17</sup>L. D. Jackel, W. H. Henkels, J. M. Warlaumont, and R. A. Buhrman, Appl. Phys. Lett. **29**, 214 (1976).  
<sup>18</sup>V. Polushkin *et al.* (unpublished).  
<sup>19</sup>S. S. Tinchev, Physica C **222**, 173 (1994).  
<sup>20</sup>J. Humlicek, J. Kircher, H.-U. Harbermeier, M. Cardona, and A. Röseler, Physica C **190**, 383 (1992).  
<sup>21</sup>See, T. Van Duzer and C. E. Turner, *Principle of Superconductive Devices and Circuits* (Elsevier, New York, 1981), p. 168. E.g., with  $t = 1.5$  nm,  $L = 30$   $\mu\text{m}$ ,  $\epsilon_r = 25$ , the stray capacitance  $C_s = 23$  fF is much smaller than the junction total capacitance (180 fF).  
<sup>22</sup>K. K. Likharev, *Dynamics of Josephson Junctions and Circuits* (Gordon and Breach, New York, 1986), p. 265.  
<sup>23</sup>G. Filatrella and N. F. Pedersen, Appl. Phys. Lett. **63**, 1420 (1993).